ORIGINAL ARTICLE

Contribution of Electrical–Thermal Aging to Slot Partial Discharge Properties of HV Motor Windings

Ailiang Kang[1] · Muqin Tian[1] · Jiancheng Song[1] · Lingyan Lin[1] · Wei Li[1] · Zhipeng Lei[1]

Abstract

During the operation of HV motor, the abrasion of stator windings because of vibration caused by electromagnetic force will lead to slot partial discharge (PD). Furthermore, the superheat induced by overcurrent or poor heat dissipation will aggravate the slot PD. To understand the developing process of slot PD and comprehend the influences of aging factors on slot PD properties, two discharge bar models were made under electrical–thermal aging. At triple the rated line-to-earth voltage of 6 kV, two stator bars were aged for 37 days under different temperatures. The slot PD was measured during different aging stages, and visual observations of the insulation and stator core surface were made at the beginning and the end of aging. The experiment results indicate that electrical–thermal aging has a significant impact on the slot PD activities. The slot PD was intense under higher thermal stress, and the surfaces of insulation and stator core were oxidized after the long-time aging. This study can provide a judging basis for fault diagnosis of HV motors.

1 Introduction

High voltage motors are one of the most important pieces of electrical equipment. Their failures are always due to electrical, thermal, environmental and mechanical stresses which interact in a synergistic way to shorten the life of the motor insulation [1]. Stator windings will vibrate at twice the power–frequency because of the huge electromagnetic force excited by power–frequency magnetic field during full-load operation [2]. The semi-conductive coating and the ground wall insulation will be abraded by the iron core under the vibration [3]. Considerable debris resulting from this vibration will clog the air ventilator and lead to thermal aging [4]. Therefore, mechanical and thermal stresses, if not well controlled, will lead to serious insulation faults. Figure 1 shows a stator bar of a 10 kV motor being removed from a stator where the semi-conductive coating and 30% of the groundwall thickness have been abraded away [5].

Various forms of PDs can occur in a motor [6]. However, due to recent improvements in the used for motor insulation, most forms of PD do little damage to the insulation materials [7]. On the other hand, some high energy discharges, such as slot PD occurring between the stator bar and the iron core surface can seriously damage the insulation [8]. Many motors are broken down after a few decades in service, due to slot partial discharge [5].

The occurrence of slot PD has been studied by many scholars. Levesque et al. [9] found that humidity cansuppress discharge activity but increase the conductivity of insulation surfaces. Stone and Maughan [10] investigated slot PD under mechanical vibration, and found that slot PD will be significant only in bars that are in the high voltage region. Song et al. [11] studied slot PD under different abrasion levels and

✉ Muqin Tian
  tianmuqin@163.com

  Ailiang Kang
  kalhyh@qq.com

  Jiancheng Song
  sjc6018@163.com

  Lingyan Lin
  llyhky@163.com

  Wei Li
  leevliwei@163.com

  Zhipeng Lei
  leizhipeng@163.com

[1] Shanxi Key Laboratory of Mining Electrical Equipment and Intelligent Control, College of Electrical and Power Engineering, Taiyuan University of Technology, Taiyuan, China

Fig. 1 A stator winding damaged from vibration abrasion

identified relationships between discharge amplitude/phase and abrasion levels. Li [12] introduced the change of slot PRPD patterns under different voltages. However, very little has been published on the relationships between slot PD characteristics and electrical–thermal aging. In this article, we analyze slot PD characteristics of stator bars taken from 6 kV/780 MVA motor. Measurements were carried out in the laboratory and phase resolved partial discharge (PRPD) patterns were obtained at various aging times, using the pulse current method compliant with IEC 60270.

2 Experimental Description

2.1 Stator Bars and Preconditioning

The groundwall insulation of the experimental bars was a modern epoxy-mica insulation system with the thickness of 2.04 mm.

The bars were subjected to preconditioning before aging was commenced. Their surfaces were checked to ensure that the semi-conductive coating was in perfect condition, and cleaned with alcohol to remove contamination. A voltage of 50 Hz was applied across each bar and gradually increased to 15 kV$_{RMS}$, in order to detect pre-existing internal defects by observing whether only typical symmetrical PRPD patterns of internal discharge occurrence [6]. The eligible bars were processed by abrading the insulation surface at the same section with the dimension of 35 mm × 30 mm × 0.7 mm and inserted into a iron core that was made up of industrial silicon steel sheets, as shown in Fig. 2.

2.2 Test Setup

The electrical–thermal accelerated aging test was performed on two 6 kV (phase-to-ground) stator bars, and the experimental work was carried out in the electromagnetic shielding room with the dimension of 10 m × 5 m × 3 m. The schematic diagram of the test setup was shown in Fig. 3.

Wherein, BPF is a band-pass filter devoted to filter out the interference signal and let the power–frequency signal pass.
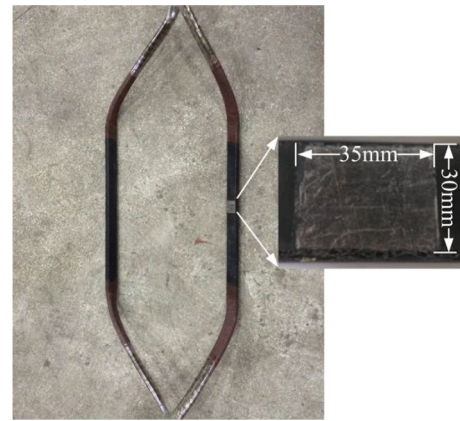

Fig. 2 One of the experiment stator bars for slot PD

LPF is a PD free isolation transformer low-pass filter which is devoted to filter the high-frequency interference mixed from the former grade equipment. T is the test transformer with the maximal PD amplitude of 0.2 pC under 100 kV. R is the water resistor of 20 kΩ which is devoted to protect the transformer T from overcurrent. Cc is a coupling capacitance of 1000 pF which produces a high-frequency path for partial discharge signal.

The highest heat-resistance temperature of F-class epoxy-mica insulation is 155 °C and the temperature of the surface insulation is about 85 °C during HV motor operating. Therefore, the experimental stator bars were divided into two groups: A and B. The aging conditions of two groups were as shown in Table 1. Wherein, the AC aging voltage is generated by a 50 Hz, 100 kV, 10 kVA test transformer. The thermal stress is generated by a heating band and PID temperature controller, which can keep the aging temperature constant.

Prior to aging, the experimental bars were annealed under 6 kV and 25 °C for 1 day, as shown in the time line in Fig. 4. At the end of stage 1, PD measurement (PD1)
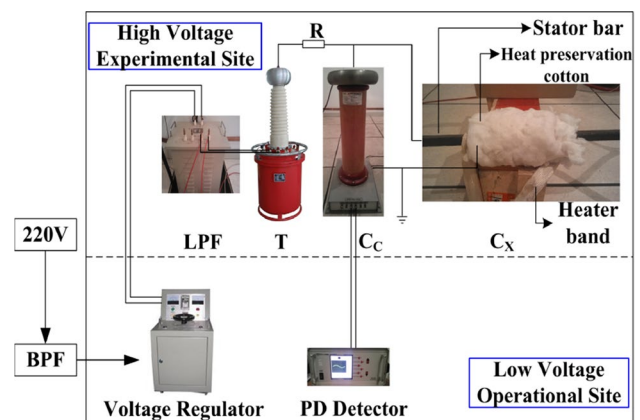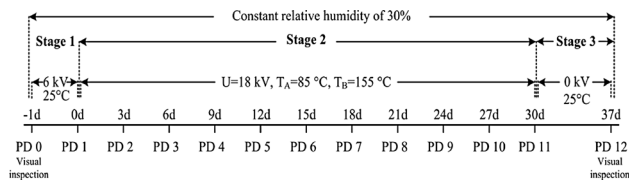

Fig. 3 Schematic diagram of the experimental system

Table 1 The experimental conditions of each groups

Group	Abrasion depth (mm)	Aging voltage (kV)	Aging temperature (°C)
A	0.7	18	85
B	0.7	18	155

Fig. 4 Time line of aging voltage and temperature for group A and group B

was carried out to investigate the influence of short-duration surface degradation. The aging of stage 2 was to accelerate the slot discharge activity by applying 18 kV and different temperatures (85 °C and 155 °C) for 30 days. During stage 3, the temperature was reduced to 25 °C for 7 days without any voltage, and the last PD (PD12) was measured. All PD measurements performed during the experiment were taken at 6 kV and relative humidity of 30%.

2.3 PD Measurement

The acquisition time for all PRPD patterns was 60 s and recordings were made at 6 kV after 30 min of conditioning, using a 1000 pF capacitive coupler in the frequency range of 80–500 kHz. PD measurements were carried out at 3-day intervals during stage 2 (0–30 days), but visual inspections of the insulation surface and the iron core surface were made only at − 1 day and at 37 day. Analysis of the PRPD patterns was through the total apparent current (NQS) in μA and discharge repetition rate in n/s and the largest discharge amplitude (Q_{max}) in pC.

3 Results

3.1 PRPD Patterns

Figure 5 shows PRPD patterns of group A measured at different aging time. The Q_{max}^+ is larger than Q_{max}^- at each of the three aging stages, and all patterns have a steep increase at the onset of the pattern during the negative voltage half-cycle. Additionally, PRPD patterns in different stages form different geometric shapes, while these geometric shapes in the same aging stage have a great similarity. The pattern

of Q^+ is like a triangle in stage 1, and the geometric shape becomes from the triangle to the quadrilateral gradually in stage 2. The differences among these PRPD patterns are due mainly to changes in the electric field in the air gap between the core and stator bar with the increase of aging time, which can shift the distribution of dominant discharge [13]. Comparing (a) and (e), the re-appearance of the triangular shape in (e) is due to the electrons trapped during stage 2 flowing to the ground [9]. However, the Q_{max}^+ is still over twice larger than that in stage 1, which proves the insulation degradation is due to the long term electrical–thermal aging.

Besides, the Q_{max}^+ is always at least $1.5 \times Q_{max}^-$, and the Q_{max}^+ increases from 9000 pC to 16,000 pC and then decreases to 12,000 pC, as can be seen in Fig. 5. The changes are assumed to be caused by the follow reasons: (1) the electrical–thermal aging can increase electronic thermal energy, which will improve the efficiency of ionizing collisions and increase the Q_{max}^+; (2) the temperature rise increases the insulation work function [17], which leads to a reduction in the availability of electrons, becoming harder to extract from the insulation surface; (3) with the long-term electrical–thermal aging, the conductivity of the insulation surface increases because of negative ions reacting during the positive voltage half-cycle [9]. The increased conductivity will increase the migration of electrons deposited on the insulation surface. With time, the electrons will spread over larger area because of the continuous increased conductivity of insulation surface, which will decrease the local field and generate smaller PD pulses; (4) the iron core is oxidized due to aging, which will decrease its conductivity and the ability of electronic emission from the iron core surface, which will lead to a small decrease in PD amplitude. The synergistic effect of the above reasons finally decrease the Q_{max}^+.

PRPD patterns of group B in different aging time are exhibited as Fig. 6. It can be seen that all patterns have a similar trend but with a higher amplitude compared with 85 °C. However, the ratio of Q_{max}^+/Q_{max}^- still remains about 1.5, which can be used as an important characteristic to judge slot discharge. Furthermore, in stage 3, the Q_{max}^+ is about 4000 pC and the geometric shape becomes quadrilateral, which is the most difference compared with group A.

3.2 Slot PD Parameters Distribution

Figure 7 shows the distribution of Q_{max} in different stages, and all curves have a similar trend, but with larger amplitude at higher temperature. The reason is that the heat produced by the heater band and the localized high temperature in the discharge area will generate thermal degradation, which will lead to a decrease of the bonding strength of the epoxy-mica interface [14]. Higher temperature can increase more electronic thermal energy and result in the slot PD activity more intense. With time, thermal degradation generates
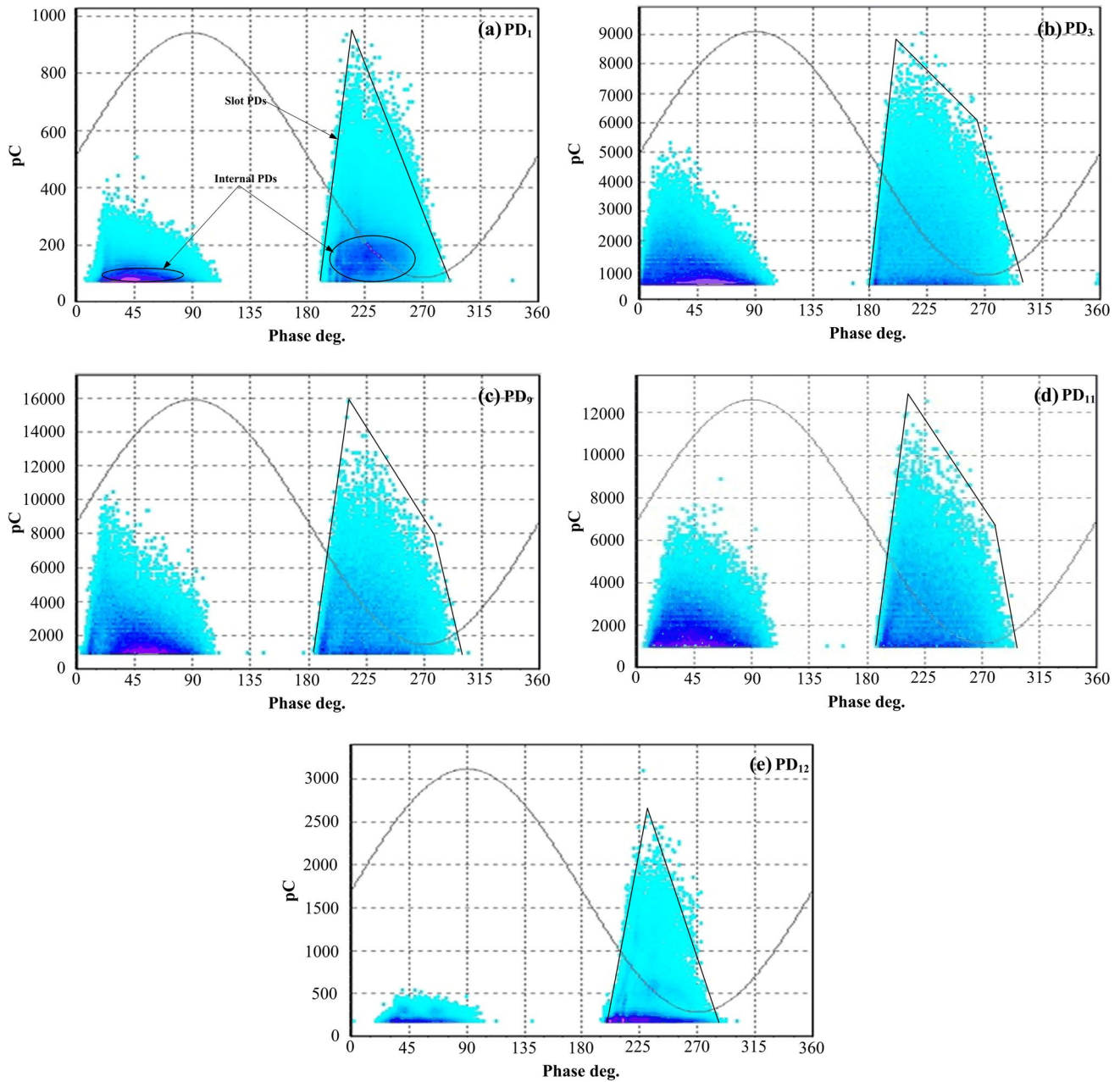
Fig. 5 PRPD patterns of group A in different stages

oxidization on the insulation surface and the iron core surface, which will lead to surface degradation and weaken the slot PD activity.

Figure 8 depicts the distribution of discharge repetition rate during stage 2. It can be clearly seen that N^- displays a trend of increased at first and then decreased gradually, while N^+ has maintained growth throughout the whole aging sequence for both two groups. However, N^+ is larger than N^- when the temperature is 85 °C, while the same condition is utterly opposite when the temperature is up to 155 °C. The main reason for this is as follows: in the experiment, we

consider 2100 pC, which is the minimum discharge amplitude, as the minimum amplitude for group A and B. In group A, lots of discharges lower than 2100 pC is filtered, which makes the N^- is less than N^+. It has been proved that slot PD is such a discharge which has smaller but more negative discharges and bigger but less positive discharges [9].

The change of initial discharge phase of group A during stage 2 is depicted as Fig. 9. The initial discharge phase of Q^- is 17° after the first aging period. With time, the initial discharge phase shifts to left and keeps constant in the 8th aging period within the scope of the 4°–5°. Q^- has the same
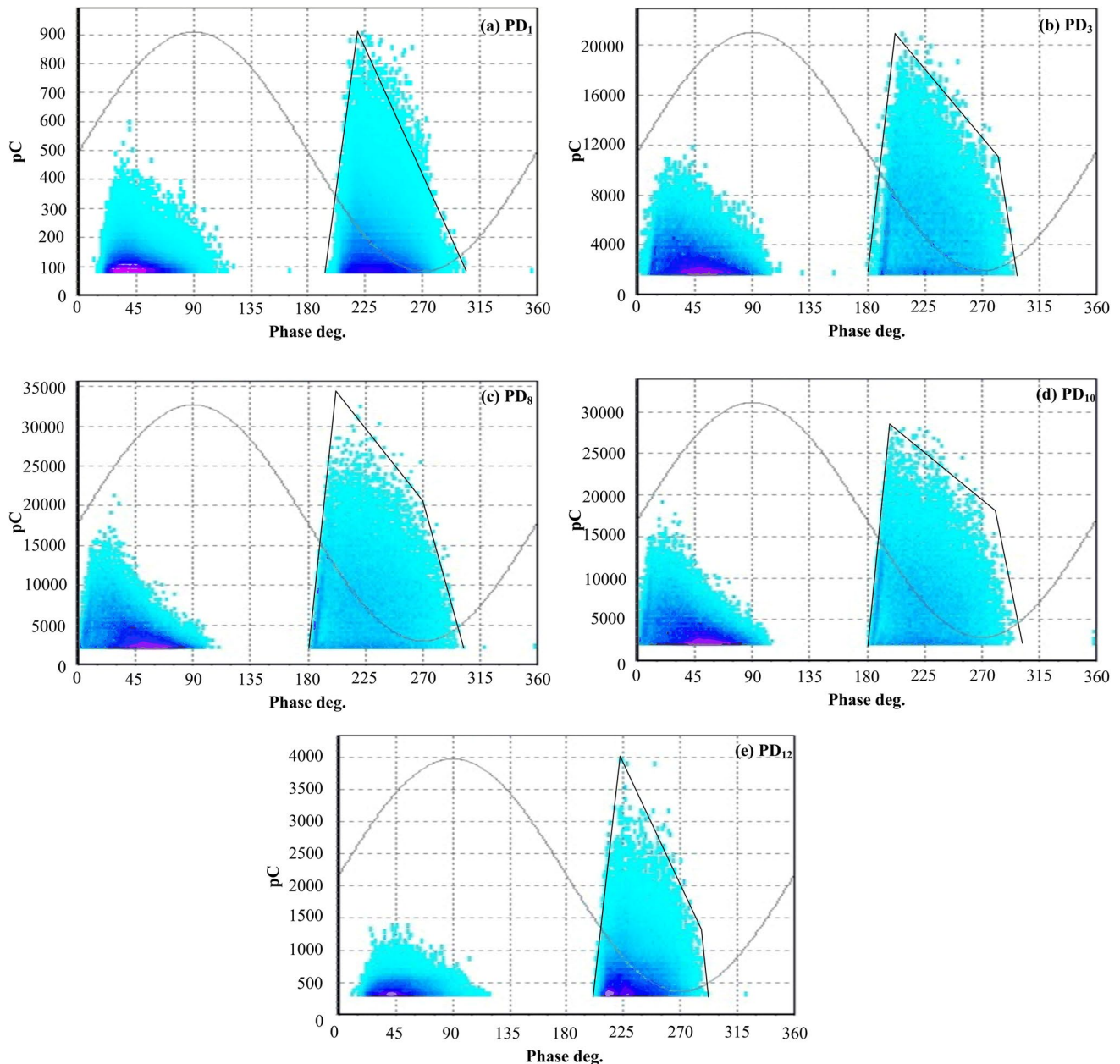
Fig. 6 PRPD patterns of group B in different stages

tendency and the initial discharge phase keeps constant in the 6th aging period within the scope of the 187°–186°. When the temperature is up to 155 °C, the initial discharge phase of Q^- and Q^+ is 1° and 180° respectively at the beginning of aging. The reason for shifting of PD inception phase can be summarized as follows: (1) electrons will be easier to gain enough thermal energy to produce a successful ionizing collision during electronic avalanche on the condition of higher temperature; (2) the modifications in the surface conditions caused by electrical–thermal aging can directly affect the electric field inside the air gap, and this field can

be much higher than the breakdown strength of air. This can explain why slot PDs are always present under higher temperature but dominant at room temperature. All the characteristics prove that electrical–thermal aging plays a crucial role in the insulation degradation.

The curves of NQS under different aging conditions are shown as Fig. 10. It is evidently demonstrated that the NQS has the trend of increase as a function of aging time and temperature. Besides, the NQS is of slow growth during stage 2. The NQS changes to 1.02 µA and 1.42 µA for group A and B in stage 3, which is still over twice than 0.54 µA in stage
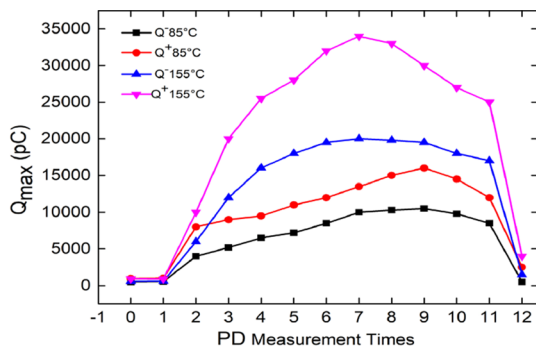
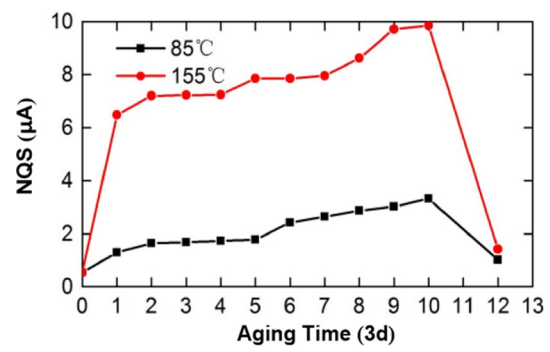**Fig. 7** Q_{max} of group A and B during different aging time
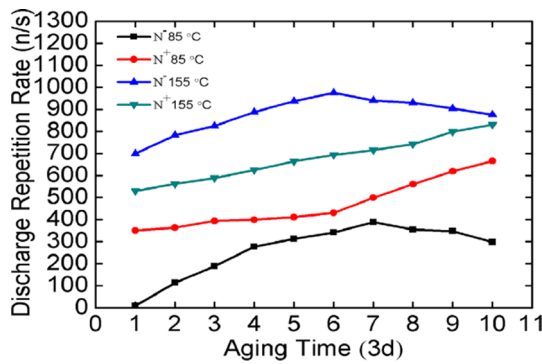
Fig. 8 Discharge repetition rate of group A and B during different aging time
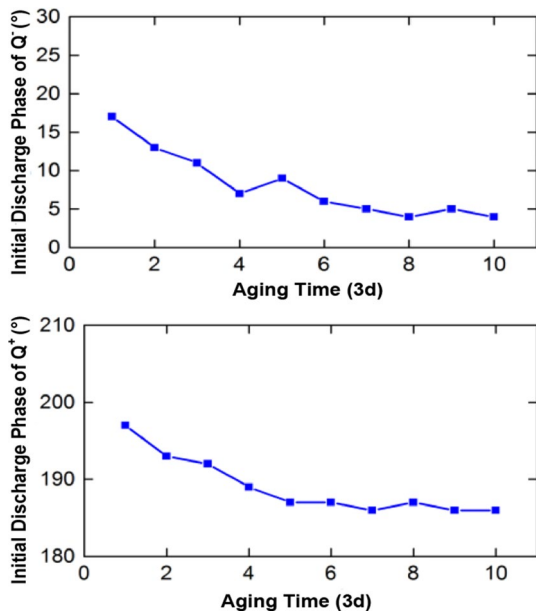
Fig. 9 The change of initial discharge phase of Q^- (top) and Q^+ (bottom) with the aging time for group A

Fig. 10 The curves of NQS under different aging temperatures and periods measured at 6 kV

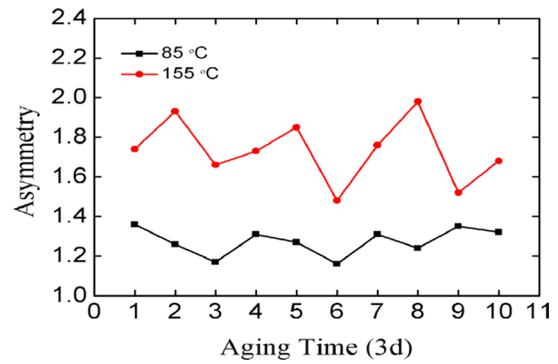**Fig. 11** The curves of Asymmetry under different aging temperatures and periods measured at 6 kV

1. The change of NQS proves that electrical–thermal aging increases the conductivity of insulation surface, which has been proved in [13].

Figure 11 shows the curves of asymmetry under different aging conditions. The ratio fluctuates between 1.15 and 1.35 when the temperature is 85 °C, and the ratio is up to 1.5–2.0 when the temperature is 155 °C. It is can be seen from the curves that slot discharge is an extremely asymmetrical discharge and the asymmetry is more obvious under a higher aging condition.

4 Discussion

The asymmetry of slot PRPD pattern has been recognized for a long time [15] and the change of signature with degradation under electrical and mechanical stresses has been published on [9], but very little has been published on the change of slot PD characteristics under electrical–thermal aging. In order to determine the role of degradation of slot PD under different conditions and the ensuing PRPD pattern changes, an accelerated aging experiment of HV motor stator bars has been carried out. With the exception of the

well-controlled electrical–thermal stress, the relative humidity is considered and kept 30% during the experiment. It is observed that electrical–thermal aging can make the insulation surface and the iron core surface degradation. Both the temperature and the surface degradation play a role in the process of slot PD activity. However, slot PD activity is more complex than initially anticipated and influenced by many factors such as the temperature of the air gap between the iron core and the insulation, the surface degradation and the electrical field. From the results presented above for different conditions of temperature and state of degradation, we have tried to infer the influence of each of these factors on the degradation mechanism of slot discharge. Analysis of the results was difficult because of the interdependence of each factor.

4.1 Slot PD Process

Before discussing the influences of mechanical abrasion, temperature and surface state on the slot discharge, it should be noted that the electrical field resulting from the phase-to-ground voltage and the field from the space charges will promote the initiation and development of the slot discharge [15]. As a result, a strong electric field, which is higher than the breakdown strength of air, is produced on this region to induce the slot discharge. In our experiment, a mock-up iron core is made to act as the cathode. During the positive voltage half-cycle, the slot discharge can be sustained because of the free electrons and the positive ions. Accordingly, series of complex reactions

take place on the iron core surface. The positive ions, once acquiring enough energy, will conquer the potential barrier and reach the core surface. Those ions will strike the core and create new free electrons and other ions. For another, free electrons will be drawn toward the insulation and trapped on its surface by the electric field, which leads to the reduction of the electrical field and make the slot discharge extinct once the field strength is reduced to the extinction field strength. Since the surface conductivity of the insulation is only about 10–16 S/square [16], surface charges will merely spread over the discharge area and electronic avalanches will be initiated in this area as well. The schematic diagram is shown as Fig. 12a.

When the voltage turns to the negative voltage half-cycle, the electric field will be higher than the breakdown strength of air due to insulation surface charges accumulating. A large number of electrons, which is deposited in the positive voltage half-cycle, will be released and become available to initiate slot discharge for the insulation surface acting as the cathode in this cycle. In this cycle, the electrons and negative ions are accelerated not only by perpendicular field toward the core but also by the tangential field toward the edge of the bar's semi-conductive coating [17]. The electrons will flow to the ground while the negative ions will oxidize the iron core once they reach the surface. Moreover, the positive ions will strike the insulation surface as well, which will degrade the insulation, reduce the electric field strength and extinguish the slot discharge. The schematic diagram is shown as Fig. 12b.

Fig. 12 The schematic diagram of slot discharge in the positive voltage half-cycle (**a**) and the negative voltage half-cycle (**b**)

(a) the positive voltage half-cycle   **(b) the negative voltage half-cycle**
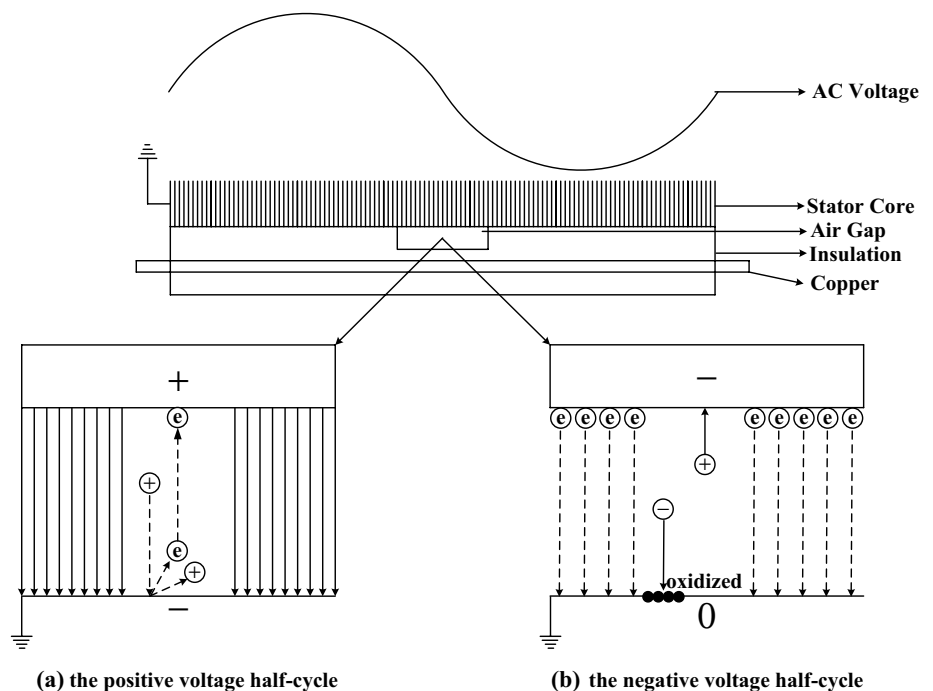
4.2 Influence of Mechanical Abrasion

Mechanical abrasion of the bar's surface is the intrinsic reason to cause slot discharge. The semi-conductive coating covered on the stator bars has the function of equalizing the potential of windings and ground. Although there is air gap between the bar and the iron core, no slot discharge occurs on condition that the semi-conductive coating is intact. However, stator windings will vibrate at twice the power–frequency because of the huge electromagnetic force during operation and the semi-conductive coating will be abraded with time, which will produce potential difference and form a strong electric field. The slot discharge takes place finally. Figure 13 shows the PRPD pattern of a stator bar without any abrasion, the most difference compared with slot discharge is that the PRPD pattern is symmetrical and the highest amplitude measured under 6 kV is 350 pC, which is much less than that of slot discharge.

4.3 Influence of Surface State

In this section, the surface state includes the stator bar surface state and the iron core surface state. The PRPD pattern of Fig. 5a was measured after annealed and barely any surface degradation occurred apart from abrasion. And there is a sharp asymmetry in the positive and the negative half-cycle for the asymmetric electric field of the metallic/insulator bounded gap. Obviously, this is not the case for non-abrasion surface, where only internal discharge occurs owing to existing small voids inside the insulation. However, after electrical–thermal aging and a sufficient recovery for winding insulation, the slot PRPD pattern is shown as Fig. 5e. The biggest difference compared with Fig. 5a is that there is a rapid increased amplitude during the negative voltage half-cycle, while during the positive voltage half-cycle, the discharge amplitude is almost no change. Since the two PRPD patterns are measured under the same voltage and temperature, the changes in PRPD patterns can be attributed to the surface degradation of both the iron core and the bar.
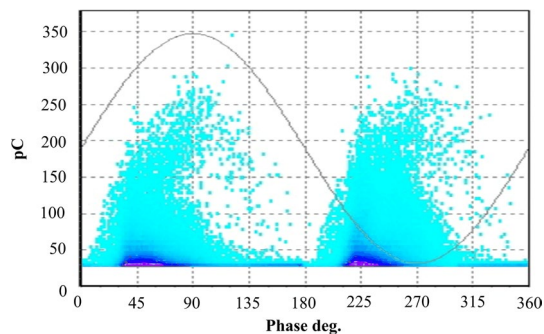
Table 2 shows the PD parameters of Fig. 5a, e, which has eliminated the internal discharge ($Q_{max} \leq 350$ pC). Obviously, very little slot discharge occurs after stage 1, especially during the positive voltage half-cycle. However, after electrical–thermal aging, the surface of insulation is degraded and the slot PD activity is easier to induced. Accordingly, the long term aging accelerate the surface degradation and promote the development of slot discharge activity.

It is a common knowledge that ozone and oxynitride will be generated as a consequence of the reactions between oxygen and nitrogen during partial discharge and these species can degrade the insulation surface and oxidize the iron core surface [9]. Figure 14 shows the changes of insulation and iron core surfaces before and after aging. Because of the heat, the insulation surface and the iron core surface

Table 2 Discharge repetition rate and NQS of group A before and after aging

Aging conditions	Before aging	After aging
N^+ (n/s)	157	1171
N^- (n/s)	4.52	595
NQS^+ (pA)	6.46×10^4	8.31×10^5
NQS^- (pA)	116	2.57×10^5
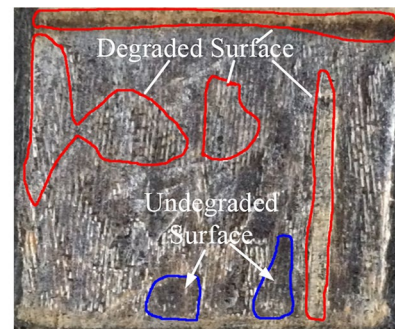
(a) The change of stator bar surface after aging
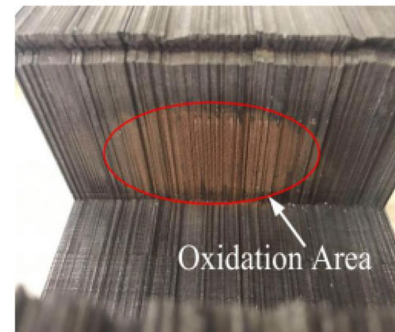
(b) The oxidation area of the iron core observed after aging

Fig. 14 The change of winding surface and stator core surface before and after aging

Fig. 13 PRPD pattern of stator bar without any abrasion measured under 6 kV

show signs of electrical–thermal aging with changes of the insulation and the iron core. The color of insulation surface becomes deeper and the iron core surface is oxidized to reddish. The oxide layer will weaken the ability of conductivity and electron emission dramatically, which will reduce the effectiveness of ionization on the iron core surface.

The availability of electron emissions from the oxidized iron core surface is reduced since the surface is more resistive as the function of aging time, slot discharge in the positive voltage half-cycle will be induced more from the edge of the abrasion area and the tangential field will become stronger and stronger, thus resulting in a higher cluster discharge in the positive voltage half-cycle as shown in Figs. 5 and 6. With time, the conductivity of insulation surface increases because of its degradation, which enhances the mobility of electrons over the area of discharge surface. Besides, the electrons will release over a larger area as the result of the increased conductivity. During the negative voltage half-cycle, the iron core acts as the anode and the electrons flow from the insulation surface to ground no matter whether the core is oxidized. In addition, other negative ions react with the iron core, which will oxidize the iron core surface and decrease its conductivity in turn.

4.4 Influence of Temperature

Many studies have clarified that temperature has a significant impact on partial discharge activities [17–19]. The well-known temperature effects are the increase in the quantities of initial electrons and ionization efficiency when the electron's thermal energy increases. On the other hand, ozone production will be reduced and nitrous oxide formation will be increased when the temperature of the air gap increases, which will lead to surface degradation [20]. Over time, surface degradation will increase the conductivity of the insulation and reduce that of the iron core, which will lower the availability of electrons and change the distribution of the electric field inside the air gap. Hence, the change of slot discharge PRPD pattern is effected by surface degradation and increase activity with temperature, and it is very difficult to determine which one of the two is more important for the change in PRPD pattern.

In the experiment conducted in our laboratory, the PD parameters of the same stage but under different aging temperatures are shown as Table 3. All parameters at 155 °C are much higher than those at 85 °C, which proves that thermal aging has a significant effect on slot PD activity. With time, the slot discharge amplitude is increased at first and then decreased, as shown in Fig. 7. The likely reason for this is that high temperature increases the electronic thermal energy and improves the efficiency of ionizing collisions. As a result, both the positive and negative discharge parameters increase. However, the oxidation of the iron

Table 3 Discharge repetition rate and NQS of PD4 for both group A and B

Aging conditions	Group A	Group B
N^+ (n/s)	411	551
N^- (n/s)	113	732
NQS^+ (pA)	1.35×10^6	3.91×10^6
NQS^- (pA)	2.92×10^5	3.14×10^6

core surface is more violent under high temperature, which decreases the ability of conductivity and electronic emission and lower the negative discharge. Nevertheless, the impact of temperature and oxidization is intertwined, which makes the discharge regularity complex and hard-to-predict. On the other hand, the asymmetry of slot discharge is increased with the increase of temperature, which is also attributed to the above reasons. In the previous study conducted by Claude Hudon [20], it has been justified that a reduction in slot discharge will take place owing to thermal expansion of stator winding under high temperature. Nevertheless, in our experiment, it has been found that the thermal expansion is less 120 μm measured by micrometer when the thermal aging of 155 °C comes to an end at once and the slot discharge is not reduced. The likely reason for these differences is that the increased discharge by ionizing collisions is much larger than the reduced discharge by thermal expansion. Therefore, temperature accelerates the intensity of slot discharge overall and the reduction of negative discharge in the preceding analysis can be neglected, especially under a higher temperature.

5 Conclusions

From the experimental investigations and analysis carried out on electrical–thermal accelerated aging of HV motor stator bars, the following conclusions can be concluded:

1. The slot PRPD patterns have different geometric shapes in different aging stages, while these geometric shapes have a great similarity in the same aging stage.
2. The slot discharge activities are increased at first and then decreased as the function of aging time and influenced by the temperature of the air gap, the surface degradation and the electrical field in a synergistic way.
3. The NQS increases gradually with time, while the growth of NQS is not linear but partitioned, and the number of partitions is increased with the increase of temperature.
4. The slot PD has an obvious asymmetry in positive and negative voltage half-cycle, and the asymmetry is more conspicuous with the increase of aging temperature.

References

1. Stone GC, Campbell SR, Sedding HG (2011) Characteristics of noise and interphasal PD pulses in operating stator windings. In: IEEE international symposium on electrical insulation conference, Annapolis, pp 15–19
2. Stone GC, Maughan CV, Nelson D, Schultz RP (2008) Impact of slot discharge and vibration sparking on stator winding life in large generators. IEEE Electr Insul Mag 24(5):14–21
3. Hudon C, Bélec M, Lévesque M (2008) Study of slot partial discharges in air-cooled generators. IEEE Trans Dielectr Electr Insul 15(6):1675–1690
4. Stone GC, Boulter EA, Culbert I, Dhirani H (2004) Electrical insulation for rotating machines. IEEE Press, Piscataway
5. Stone GC, Wu R (2009) Examples of stator winding insulation deterioration in new generators. In: IEEE 9th international conference properties and applications of dielectric materials, Harbin, pp 883–886
6. Hudon C, Bélec M (2005) Partial discharge signal interpretation for generator diagnostics. IEEE Trans Dielectr Electr Insul 12(2):297–319
7. Younsi K, Snopek D, Hayvard J, Menard P, Pellerin JC (2001) Seasonal changes in partial discharge activity on hydraulic generators. In: IEEE electrical insulation conference and electrical manufacturing and coil winding, Cincinnati, pp 423–428
8. Rüdiger S, Laird T, Watters C (2008) Case study using an additional neutral point PD sensor for generator stator monitoring. In: IEEE international symposium on electrical insulation, Vancouver, pp 551–557
9. Lévesque M, David E, Hudon C, Bélec M (2012) Contribution of humidity to the evolution of slot partial discharges. IEEE Trans Dielectr Electr Insul 19(1):61–75
10. Stone GC, Maughan C (2008) Vibration sparking and slot discharge in stator windings. In: IEEE international symposium on electrical insulation, pp 148–152
11. Song J, Li C, Lin L (2013) Slot discharge pattern of 10 kV induction motor stator coils under condition of insulation degradation. IEEE Trans Dielectr Electr Insul 20(6):2091–2098
12. Li C, Song J, Kang A et al (2014) PD patterns of stator windings by in-factory experiment on a 10 kV motor. In: IEEE international symposium on electrical insulation material, pp 168–171
13. Lévesque M, David É, Hudon C, Bélec M (2010) Effect of surface degradation on slot partial discharge activity. IEEE Trans Dielectr Electr Insul 17(5):1428–1440
14. Las T (2000) Measurement of solid dielectric surface temperature increment arising from partial discharge activity. In: IEEE international symposium on electrical insulation, Anaheim, pp 324–327
15. Jackson RJ, Wilson A (1982) Slot-discharge activity in air-cooled motors and generators. IEE Proc 129(3):159–167
16. Breen HJ, Gulski E, Smit JI, Verhaart H, Leeuw W (2002) The importance on generator operating conditions on PD data evaluation. In: IEEE international symposium on electrical insulation, Boston, pp 582–585
17. Schifani R, Candela R, Romano P (2001) On PD mechanisms at high temperature in voids included in an epoxy resin. IEEE Trans Dielectr Electr Insul 8(4):589–597
18. Odic E, Jouseau E, Vivien G, Maroni CS (2006) Characterization of medium voltage equipment ageing by monitoring of partial discharges chemical and acoustical emission. In: 10th International electrical insulation conference, Birmingham, pp 24–29
19. Li C, Hu J, Lin C, He J (2017) The potentially neglected culprit of DC surface flashover: electron migration under temperature gradients. Sci Rep 7:3271
20. Hudon C, Chaaban M, Belec M, Nguyen DN (2007) Effect of temperature and thermal expansion on slot PD activity. In: Electrical insulation conference and electrical manufacturing expo, pp 122–126

Ailiang Kang was born in Hebei, China in 1988. He received the B.Sc. degree and the M.Sc. Degree from the Taiyuan University of Technology, China in 2013 and 2016, respectively. Currently, he is a Ph.D. candidate in the College of Electrical and Power Engineering, Taiyuan University of Technology. His research interests include PD measurement for rotating machines, PD sources identification and localization for HV motors and generators.

Muqin Tian was born in Shanxi, China, in June 1962. She received the B.S. degree from Dalian Railroad Institute, China, in 1987, the M.S. degree from Taiyuan University of Technology, China, in 1990, and the Ph.D. degree from Taiyuan University of Technology, China, in 2006. Her main interest is state monitoring and early warning of large mechanical equipment and intelligent control. Currently, she is director of the Department of Electrical Engineering at Taiyuan University of Technology.

Jiancheng Song (M'13) received the B.Sc. degree from Taiyuan University of Technology, China, in 1982, the M.Sc. degree from Newcastle University, England, in 1987, respectively and the Ph.D. degree from Xi'an Jiaotong University, China, in 1999. Currently, he is a professor of the College of Electrical and Power Engineering at Taiyuan University of Technology. He has experience in the field of condition assessment, remaining life assessment and intellectual automation technology. He has performed a number of electrical failure investigations about coal mine. He has presented a number of technical and scientific papers at international conferences and seminars.

Lingyan Lin was born in Shanxi, China, on 16 August 1969. She received the B.S. degree from Taiyuan University of Technology, China, in 1991, the M.S. degree from Taiyuan University of Technology, China, in 1994. the Ph.D. Degree from Taiyuan University of Technology, China, in 2014. Currently, she is an associate professor of the College of Electrical and Power Engineering at Taiyuan University of Technology. Her main research interest is condition assessment of HV motor failure and associated PD characteristics, intelligence techniques.

Zhipeng Lei was born in Taiyuan, China in 1983. He received the B.Sc. degree from the East China Jiaotong University, China in 2005, and the M.Sc. degree and Ph.D. degree from the Taiyuan University of Technology, China in 2010 and 2015, respectively. He joined the College of Electrical and Power Engineering in the Taiyuan University of Technology as a lecturer since 2015. His main research interest is condition assessment of high voltage cable failure and associated partial discharges characteristics, intelligence techniques in coal mine.

Wei Li was born in Shanxi, China, on 8 February 1994. She received the B.S. degree from Henan Polytechnic University, China in 2016. Right now she has been studying in Taiyuan University of Technology to receive her M.S. degree since 2017. Her main research interest is the PD recognition for HV motors.